 CMES, vol.41, no.3, pp.215-241, 2009

Elastic transient analysis with MLPG(LBIE) method and local RBFs

E. J. Sellountos[1], **A. Sequeira**[1] **and D. Polyzos**[2]

Abstract: A Meshless Local Petrov-Galerkin (MLPG) method based on Local Boundary Integral Equation (LBIE) techniques is employed here for the solution of transient elastic problems with damping. The Radial Basis Functions (RBF) interpolation scheme is exploited for the meshless representation of displacements throughout the computational domain. On the intersections between the local domains and the global boundary, tractions are treated as independent variables via conventional boundary interpolation functions. The MLPG(LBIE)/RBF method is applied to both transient and steady-state Fourier transform elastodynamic domains. In both cases the LBIEs employ the simple elastostatic fundamental solution instead of the complicated time and frequency dependent ones. The transient version of the present MLPG(LBIE)/RBF technique utilizes the θ-Wilson finite difference scheme for the treatment of acceleration and velocity terms, while the frequency domain formulation exploits the Fast Fourier Transform (FFT) for the conversion of frequency domain solutions into time domain fields. The accuracy of the proposed methodology is assesed with three representative numerical examples.

Keywords: Meshless methods, Meshless Local Petrov-Galerkin (MLPG), Local Boundary Integral Equation (LBIE), elastodynamic transient analysis, elastodynamic steady-state analysis

1 Introduction

The Boundary Element Method (BEM) is a very well known and robust method for solving elastodynamic problems [Beskos (1987), Beskos (1997)]. However, in its conventional time-domain form it uses the elastodynamic fundamental solution, which increases the computational effort in transient problems, due to its complicated form [Manolis and Beskos (1988), Dominguez (1993)]. The use of the much

[1] Instituto Superior Técnico, Technical University of Lisbon, CEMAT/IST, Lisbon, Portugal.
[2] University of Patras, Department of Mech. Engineering and Aeronautics, Patras-Rion, Greece.

simpler elastostatic fundamental solution creates an inertia volume integral, which requires an interior discretization in addition to the boundary mesh. A solution to this problem is offered by the Dual Reciprocity BEM (DR/BEM) proposed by [Nardini and Brebbia (1983)] where the inertia volume terms are transformed into boundary integrals. This method, although elegant as a boundary approach, is not maybe the best for time-domain applications due to its convergence problems [Agnantiaris, Polyzos, and Beskos (1998)]. Another approach is the conversion of the transient problem into a steady-state one through Fourier or Laplace Transform, then solution of the problem in the transformed domain [Polyzos, Tsinopoulos, and Beskos (1998)] and inversion of the obtained results into time-domain via inverse Fourier [Kausel and Roësset (1992)] or Laplace [Durbin (1974), Manolis and Beskos (1981)] transform algorithms. The problems in this case is the numerical treatment of the complex harmonic fundamental solution and the computationally expensive fully populated final system of algebraic equations.

To circumvent this kind of problems, Atluri and co-workers proposed the Local Boundary Integral Equation (LBIE) method [Zhu, Zhang, and Atluri (1998)] and the Meshless Local Petrov-Galerkin (MLPG) method [Atluri and Zhu (1998)] as alternatives to the BEM and FEM, respectively. Both methods are characterized as "truly meshless" since no background cells are required for the numerical evaluation of the involved integrals. Properly distributed nodal points, without any connectivity requirement, covering the domain of interest as well as the surrounding global boundary are employed instead of any boundary or finite element discretization. All nodal points belong to regular sub-domains (e.g. circles for two-dimensional problems) centered at the corresponding collocation points. The fields at the local and global boundaries as well as in the interior of the subdomains are usually approximated by the Moving Least Squares (MLS) approximation scheme. Owing to regular shapes of the sub-domains, both surface and volume integrals are easily evaluated. The local nature of the sub-domains leads to a sparse linear system of equations.

Depending on the weak formulation's test functions of the MLPG method, Atluri and coworkers developed six different MLPG methodologies numbered from one to six [Atluri and Shen (2002a); Atluri and Shen (2002b)]. The MLPG4 method utilizes as test functions, the fundamental solution of the differential equation (or part of the differential equation) of the problem, resulting into a MLPG approach equivalent to the LBIE method. For this reason, in the present work the LBIE method is called MLPG(LBIE) method.

Several papers dealing with MLPG(LBIE) solutions of linear elastic problems have appeared in the literature. The most representative are those of [Atluri, Sladek, Sladek, and Zhu (2000); Sladek, Sladek, Atluri, and Keer (2000); Sladek, Sladek,

and Keer (2003); Sladek, Sladek, and Atluri (2002); Atluri, Han, and Shen (2003); Han and Atluri (2003); Sellountos and Polyzos (2003); Sellountos and Polyzos (2005a); Sellountos and Polyzos (2005b); Sellountos, Vavourakis, and Polyzos (2005); Bodin, Ma, Xin, and Krishnaswami (2006); Vavourakis, Sellountos, and Polyzos (2006); Han and Atluri (2007); Vavourakis and Polyzos (2007); Vavourakis and Polyzos (2008); Vavourakis (2008);] while a comprehensive presentation on the application of the MLPG(LBIE) method to different types of boundary value problems can be found in the review paper of [Sladek, Sladek, and Atluri (2002)] and in the book of [Atluri (2004)].

In the context of transient analysis, first [Sladek, Sladek, and Keer (2003)] employed the conventional MLPG(LBIE) method with the MLS approximation scheme and solved transient elastic problems working in both time and Laplace transform domains. The main problem with their methodology was the use of derivatives of MLS approximation functions in the approximation of the boundary traction vectors, a fact that affects negatively the accuracy of the MLPG(LBIE) method as it is pointed out in [Vavourakis, Sellountos, and Polyzos (2006)]. Later, [Sellountos and Polyzos (2005b)] proposed a new MLPG (LBIE) method for solving transient linear elastic problems. The main characteristic of this work was the use of relatively uniform distribution of nodal points, so in the global boundary, the MLS interpolation scheme possesses the δ-property [Gosz and Liu (1996)] and the essential boundary conditions can be imposed directly on the fictitious nodal displacements and tractions. Its advantage, as it is compared to the work of [Sladek, Sladek, and Keer (2003)] was the treatment of boundary displacements and tractions as independent variables avoiding the derivatives of MLS approximation functions. Although accurate, the requirement of relatively uniform distribution of nodal points throughout the analyzed domain confines the use of the method to structures with regular shapes.

One of the most important issues in meshless methods is the choice of the proper interpolation functions used for the representation of the analyzed fields [Sladek, Sladek, and Tanaka (2005); Sladek, Sladek, and Zhang (2006); Vavourakis, Sellountos, and Polyzos (2006); Sladek, Sladek, and Zhang (2008)]. After the MLS approximation, the most frequently used interpolation scheme is the RBF [Libre, Emdadi, Kansa, Shekarchi, and Rahimian (2008); Kosec and Sarler (2008); Le, Mai-Duy, Tran-Cong, and Baker (2008); Orsini, Power, and Morvan (2008); Ma (2008)]. Very recently [Sellountos and Sequeira (2008b); Sellountos and Sequeira (2008a)] developed an MLPG(LBIE) method for the solution of two-dimensional incompressible fluid flows. The method was based on an efficient Radial Basis Functions (RBF) scheme for the interpolation of the interior and boundary variables. The inverse matrix of the RBF was computed only once for every nodal point

and the interpolation functions were evaluated by the inner product of the inverse matrix with the weight vector associated to the integration point. This technique leads to a fast and efficient meshless approach, where the locality of the method is maintained and the system matrices are banded with small bandwidth. In the present work a new MLPG(LBIE)-RBF methodology for solving transient elastic problems is presented. On the global boundary, tractions are treated as independent variables via conventional boundary interpolation functions. The proposed method is applied to both transient and steady-state Fourier transform elastodynamic domains. In both cases the LBIEs employ the simple elastostatic fundamental solution instead of the complicated time dependent or frequency dependent one. The transient version of the present MLPG(LBIE)-RBF technique uses the θ-Wilson [Bathe (1996)] finite difference scheme for the treatment of acceleration and velocity terms, while the frequency domain formulation exploits the Fast Fourier Transform (FFT) for the conversion of frequency domain solutions into time domain fields. The paper is organized as follows: in the next section the RBF interpolation scheme is illustrated. Sections 3 and 4 explain the MLPG(LBIE) formulation in time and Fourier transform domains, respectively. Finally in section 5, three benchmarks are provided to demonstrate the accuracy of the proposed method.

2 RBF interpolation scheme

In this section the RBF interpolation scheme exploited in the present paper is illustrated. More details one can find in the book of [Atluri (2004)] and in the works of [Wang and Liu (2002b), Wang and Liu (2002a)]. Recent works employing RBFs on meshless methods are those of [Wen, Aliabadi, and Liu (2008); Kosec and Sarler (2008); Mohammadi (2008); Emdadi, Kansa, Libre, Rahimian, and Shekarchi (2008); Libre, Emdadi, Kansa, Rahimian, and Shekarchi (2008)] and [Orsini, Power, and Morvan (2008)]. Consider an elastic domain Ω surrounded by a boundary Γ covered by arbitrary distributed points $\mathbf{y}_j$, as shown in Fig. 1. Each point is considered as the center of a small circular domain Ω_j of radius r_j, called support domain of $\mathbf{y}_j$. All support domains of the adjacent nodal points $\mathbf{y}_k$, satisfying the condition

$$\left|\mathbf{y}_k - \mathbf{y}_j\right| < r_k + r_j \tag{1}$$

form a domain called domain of influence of point $\mathbf{y}_j$ (Fig. 1). At any integration point $\mathbf{x}$ (Fig. 1), the interpolation of the unknown displacement field is accomplished by the relation

$$u(\mathbf{x}) = \sum_{i=1}^{n} B_i a_i + \sum_{l=1}^{m} P_l b_l = \mathbf{B}^T\left(\mathbf{y}^k, \mathbf{x}\right) \cdot \mathbf{a} + \mathbf{P}^T(\mathbf{x}) \cdot \mathbf{b} \tag{2}$$

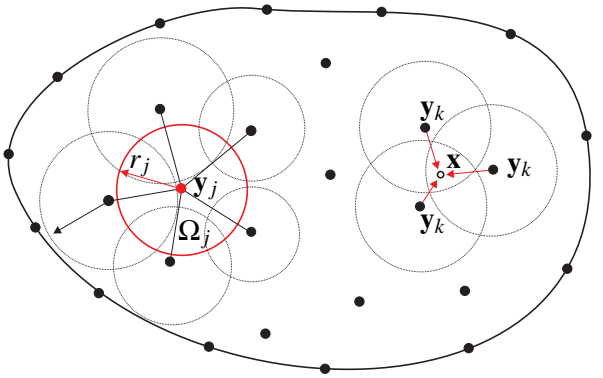

Figure 1: Domain of influence of the point $\mathbf{y}_j$ and domain of definition $\mathbf{y}_k$ of point $\mathbf{x}$

where n is the total number of the nodal points belonging to the domain of definition of point $\mathbf{x}$ and m is the degree of the polynomial basis used for the interpolation. For linear basis, m is equal to 3, while for quadratic basis, m is equal to 6. $\mathbf{B}(\mathbf{x})$ is the RBF vector with dimension $n \times 1$ and $\mathbf{P}(\mathbf{x})$ is a monomial basis vector with dimension $m \times 1$. Finally, both $\mathbf{a}$ and $\mathbf{b}$ are unknown vectors with dimensions $n \times 1$ and $m \times 1$, respectively, that depend on the location of the adjacent points of the domain of definition $\mathbf{y}_k$ of point $\mathbf{x}$. More precisely the vector $\mathbf{B}\left(\mathbf{y}^k, \mathbf{x}\right)$ has the form

$$\mathbf{B}\left(\mathbf{y}^k, \mathbf{x}\right) = \begin{bmatrix} W(\mathbf{y}_1, \mathbf{x}) \\ W(\mathbf{y}_2, \mathbf{x}) \\ \dots \\ W(\mathbf{y}_n, \mathbf{x}) \end{bmatrix}_{n \times 1} , k = 1, \dots, n \tag{3}$$

where W represents a prescribed radial function. In the present work multiquadric radial functions are employed and thus W has the form

$$W(\mathbf{y}, \mathbf{x}) = \left(r^2 + Q^2\right)^{0.5} \tag{4}$$

where $r = |\mathbf{y} - \mathbf{x}|$ is the distance between the two points and Q is a nodal parameter, the optimal value of which is determined to be equal to [Hardy (1990)]

$$Q(\mathbf{x}) = 0.815 \frac{1}{n} \sum_{i=1}^{n} d_i \tag{5}$$

where d_i is the distance between every point $\mathbf{y}_k$ in the domain of definition of the point $\mathbf{x}$ and its closest nodal neighbor. The polynomial vector $\mathbf{P}$ has the form

$$\mathbf{P}^T(\mathbf{x}) = \left[\begin{array}{ccc} 1 & x & y \end{array}\right]_{1\times m} \tag{6}$$

for linear basis and

$$\mathbf{P}^T(\mathbf{x}) = \left[\begin{array}{cccccc} 1 & x & y & x^2 & xy & y^2 \end{array}\right]_{1\times m} \tag{7}$$

for the quadratic basis. The determination of the unknown vectors $\mathbf{a}(\mathbf{y}_k)$ and $\mathbf{b}(\mathbf{y}_k)$ is accomplished by constructing a set of equations that impose an interpolation passing through all nodal points belonging to the domain of definition of $\mathbf{y}_k$

$$u(\mathbf{y}_e) = \sum_{i=1}^{n} B_i(\mathbf{y}_k, \mathbf{y}_e)\, a_i + \sum_{l=1}^{m} P_l(\mathbf{y}_e)\, b_l. \tag{8}$$

Where $\mathbf{y}_e, e = 1,...,n$ are the interpolation nodal points in the domain of definition of point $\mathbf{x}$. In addition to the previous relation the following equation is taken into account [Wang and Liu (2002a)]

$$\sum_{j=1}^{n} P_l(\mathbf{y}_k)\, a_j(\mathbf{y}_k) = 0, \qquad l = 1,..,m \tag{9}$$

and the following system of equations is formed

$$\left[\begin{array}{cc} \mathbf{B_0} & \mathbf{P_0} \\ \mathbf{P_0}^T & \mathbf{0} \end{array}\right]_{(n+m)\times(n+m)} \left[\begin{array}{c} \mathbf{a} \\ \mathbf{b} \end{array}\right]_{n+m} = \left[\begin{array}{c} \mathbf{u} \\ \mathbf{0} \end{array}\right]_{n+m} \tag{10}$$

or

$$\mathbf{A}(\mathbf{y}_k) \left[\begin{array}{c} \mathbf{a} \\ \mathbf{b} \end{array}\right] = \left[\begin{array}{c} \mathbf{u} \\ \mathbf{0} \end{array}\right]. \tag{11}$$

The matrix $\mathbf{A}(\mathbf{y}_k)$ is symmetric and consists of the submatrices $\mathbf{B}_0(\mathbf{y}_k)$ and $\mathbf{P}_0(\mathbf{y}_k)$ that depend on the nodal points $\mathbf{y}_k$, and have the following form

$$\mathbf{B}_0(\mathbf{y}_k) = \left[\begin{array}{c} \mathbf{B}^T(\mathbf{y}_k, \mathbf{y}_1) \\ \mathbf{B}^T(\mathbf{y}_k, \mathbf{y}_2) \\ \cdots \\ \mathbf{B}^T(\mathbf{y}_k, \mathbf{y}_n) \end{array}\right]_{n\times n} \tag{12}$$

or

$$\mathbf{B}_0 = \left[\begin{array}{cccc} W(\mathbf{y}_1, \mathbf{y}_1) & W(\mathbf{y}_2, \mathbf{y}_1) & \cdots & W(\mathbf{y}_n, \mathbf{y}_1) \\ W(\mathbf{y}_1, \mathbf{y}_2) & W(\mathbf{y}_2, \mathbf{y}_2) & \cdots & W(\mathbf{y}_n, \mathbf{y}_2) \\ \cdots & \cdots & \cdots & \cdots \\ W(\mathbf{y}_1, \mathbf{y}_n) & W(\mathbf{y}_2, \mathbf{y}_n) & \cdots & W(\mathbf{y}_n, \mathbf{y}_n) \end{array}\right]_{n\times n} \tag{13}$$

and

$$\mathbf{P}_0(\mathbf{y}_k) = \begin{bmatrix} \mathbf{P}^T(\mathbf{y}_1) \\ \mathbf{P}^T(\mathbf{y}_2) \\ \cdots \\ \mathbf{P}^T(\mathbf{y}_n) \end{bmatrix}_{n\times m} . \tag{14}$$

Finally Eq. 2 is written in the form

$$u(\mathbf{x}) = \begin{bmatrix} \mathbf{B}^T(\mathbf{x}) & \mathbf{P}^T(\mathbf{x}) \end{bmatrix} \mathbf{A}^{-1}(\mathbf{y}_k) \begin{bmatrix} \mathbf{u}(\mathbf{y}_k) \\ \mathbf{0} \end{bmatrix} = R(\mathbf{x})\,\mathbf{u}(\mathbf{y}_k) \tag{15}$$

with

$$R^k(\mathbf{x}) = \sum_{i=1}^{n} B_i(\mathbf{x}) A^{-1}_{i,k}(\mathbf{y}_k) + \sum_{l=1}^{m} P_l(\mathbf{x}) A^{-1}_{n+l,k}(\mathbf{y}_k) \tag{16}$$

representing the interpolation functions adopted in the present work. The derivatives of the interpolation functions can be derived by differentiating Eq. 16 with respect to the spatial coordinates x, y

$$\begin{aligned} \frac{\partial R^k(\mathbf{x})}{\partial x} &= \sum_{i=1}^{n} \frac{\partial B_i(\mathbf{x})}{\partial x} A^{-1}_{i,k}(\mathbf{y}_k) + \sum_{l=1}^{m} \frac{\partial P_l(\mathbf{x})}{\partial x} A^{-1}_{n+l,k}(\mathbf{y}_k) \\ \frac{\partial R^k(\mathbf{x})}{\partial y} &= \sum_{i=1}^{n} \frac{\partial B_i(\mathbf{x})}{\partial y} A^{-1}_{i,k}(\mathbf{y}_k) + \sum_{l=1}^{m} \frac{\partial P_l(\mathbf{x})}{\partial y} A^{-1}_{n+l,k}(\mathbf{y}_k) . \end{aligned} \tag{17}$$

3 Direct time domain MLPG(LBIE) formulation

Consider a two-dimensional linear and isotropic elastic domain Ω surrounded by a surface Γ part of which is subjected to an exterior transient excitation (Fig. 2). Then, at any point $\mathbf{y}$ of the body, the displacement vector $\mathbf{u}$ satisfies the Navier-Cauchy partial differential equation [Manolis and Beskos (1988); Dominguez (1993)]:

$$\mu\nabla^2\mathbf{u}(\mathbf{y},t) + (\lambda+\mu)\nabla\nabla\cdot\mathbf{u}(\mathbf{y},t) + \mathbf{b}(\mathbf{y},t) = \rho\ddot{\mathbf{u}}(\mathbf{y},t) \tag{18}$$

where λ μ and ρ stand for the Lamé constants and the mass density, respectively, $\mathbf{b}$ indicates body forces, ∇ is the gradient operator and dots indicate differentiation with respect to time t. In case where $\mathbf{b}$ represents damping forces, Eq. 18 takes the form

$$\mu\nabla^2\mathbf{u}(\mathbf{y},t) + (\lambda+\mu)\nabla\nabla\cdot\mathbf{u}(\mathbf{y},t) = \rho\ddot{\mathbf{u}}(\mathbf{y},t) + \zeta\dot{\mathbf{u}}(\mathbf{y},t) \tag{19}$$

where ζ is a damping coefficient. The boundary conditions are assumed to be

$$\begin{aligned} \mathbf{u}(\mathbf{y},t) &= \bar{\mathbf{u}}(\mathbf{y},t), \mathbf{y} \in \Gamma_u \\ \mathbf{t}(\mathbf{y},t) &= \bar{\mathbf{t}}(\mathbf{y},t), \mathbf{y} \in \Gamma_t \end{aligned} \tag{20}$$

with $\mathbf{t}$ denoting the traction vector, $\bar{\mathbf{u}}, \bar{\mathbf{t}}$ represent prescribed vectors and $\Gamma_u \cup \Gamma_t \equiv \Gamma$.

Considering the static fundamental solution of Eq. 19 and employing the Betti's

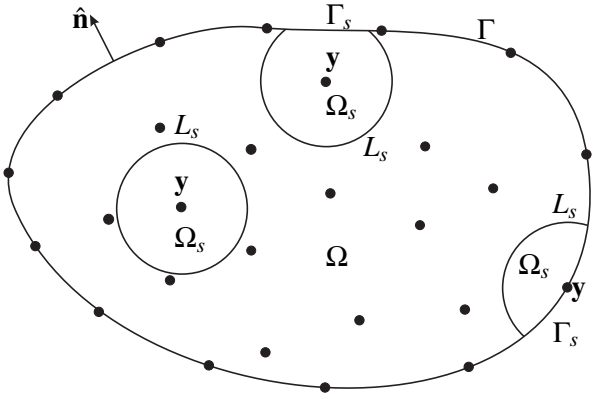

Figure 2: Local domains and local boundaries used for the local integral representation of displacements at the point $\mathbf{y}$.

reciprocal identity, one obtains the following LBIE for the circular domain centered at any interior or boundary point $\mathbf{y}$ (Fig. 2).

$$\begin{aligned} \alpha \mathbf{u}(\mathbf{y},t) + \int_{\Gamma_s \cup L_s} \mathbf{t}^*(\mathbf{y},\mathbf{x}) \cdot \mathbf{u}(\mathbf{x},t)\, d\Gamma_x = \int_{\Gamma_s \cup L_s} \mathbf{u}^*(\mathbf{y},\mathbf{x}) \cdot \mathbf{t}(\mathbf{x},t)\, d\Gamma_x - \\ \rho \int_{\Omega_s} \mathbf{u}^*(\mathbf{y},\mathbf{x}) \cdot \ddot{\mathbf{u}}(\mathbf{x},t)\, d\Omega_x - \zeta \int_{\Omega_s} \mathbf{u}^*(\mathbf{y},\mathbf{x}) \cdot \dot{\mathbf{u}}(\mathbf{x},t)\, d\Omega_x \end{aligned} \tag{21}$$

where α is equal to 1 for internal points and $1/2$ for points lying on the smooth global boundary Γ. $\mathbf{u}^*, \mathbf{t}^*$ represent the fundamental displacement and traction tensors, respectively, given in [Polyzos, Tsinopoulos, and Beskos (1998)], having the form

$$\mathbf{u}^* = \frac{1}{8\pi\mu(1-\nu)} \left[(4\nu - 3) \log r \mathbf{I} + \hat{\mathbf{r}} \otimes \hat{\mathbf{r}} \right] \tag{22}$$

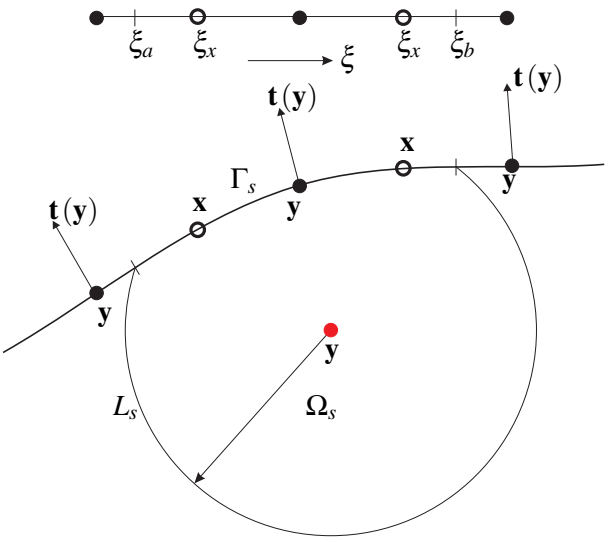

Figure 3: Quadratic or linear interpolation of boundary tractions $\mathbf{t}(\mathbf{x})$ defined on local boundaries Γ_s, using only boundary nodes

$$\mathbf{t}^* = \frac{1}{2\pi}\left[\frac{1-2\nu}{2r(-1+\nu)}\left((\hat{\mathbf{r}}\cdot\hat{\mathbf{n}})\,\mathbf{I}+\hat{\mathbf{n}}\otimes\hat{\mathbf{r}}\right)+\frac{1}{2r(1-\nu)}\left(\hat{\mathbf{r}}\otimes\hat{\mathbf{n}}-2\hat{\mathbf{r}}\otimes\hat{\mathbf{r}}\,(\hat{\mathbf{r}}\cdot\hat{\mathbf{n}})\right)+\right.$$
$$\left.\frac{\nu}{r(-1+\nu)}\hat{\mathbf{r}}\otimes\hat{\mathbf{n}}\right] \tag{23}$$

with $\mathbf{r}=\mathbf{x}-\mathbf{y}$, $\hat{\mathbf{r}}=\mathbf{r}/r$ and $\hat{\mathbf{n}}$ being the vector normal to the boundary Γ. In order to get rid of traction vectors appearing in integrals defined on L_s, the use of the companion solution $\mathbf{u}^c$ is made [Atluri, Sladek, Sladek, and Zhu (2000)]. Thus the LBIE Eq. 21 takes the form

$$\begin{aligned}\alpha\mathbf{u}(\mathbf{y},t)+\int_{\Gamma_s\cup L_s}\left[\mathbf{t}^*(\mathbf{y},\mathbf{x})-\mathbf{t}^c(\mathbf{y},\mathbf{x})\right]\cdot\mathbf{u}(\mathbf{x},t)\,d\Gamma_x=\\ \int_{\Gamma_s}\left[\mathbf{u}^*(\mathbf{y},\mathbf{x})-\mathbf{u}^c(\mathbf{y},\mathbf{x})\right]\cdot\mathbf{t}(\mathbf{x},t)\,d\Gamma_x-\\ \rho\int_{\Omega_s}\left[\mathbf{u}^*(\mathbf{y},\mathbf{x})-\mathbf{u}^c(\mathbf{y},\mathbf{x})\right]\cdot\ddot{\mathbf{u}}(\mathbf{x},t)\,d\Omega_x-\\ \zeta\int_{\Omega_s}\left[\mathbf{u}^*(\mathbf{y},\mathbf{x})-\mathbf{u}^c(\mathbf{y},\mathbf{x})\right]\cdot\dot{\mathbf{u}}(\mathbf{x},t)\,d\Omega_x\end{aligned} \tag{24}$$

where

$$\mathbf{u}^c = \frac{1}{2\pi\mu}\left[\Psi\mathbf{I} + X\hat{\mathbf{r}}\otimes\hat{\mathbf{r}}\right]$$
$$X = \frac{1}{4(1-\nu)}\frac{r^2}{r_0^2}\hat{\mathbf{r}}\otimes\hat{\mathbf{r}}$$
$$\Psi = \frac{1}{4(1-\nu)}\left[\frac{5-4\nu}{2(3-4\nu)}\left(1-\frac{r^2}{r_0^2}\right)+(4\nu-3)\ln r_0\right] \tag{25}$$

$$\mathbf{t}^c = \frac{1}{2\pi}\left[\left(\frac{d\Psi}{dr}-\frac{X}{r}\right)\left((\hat{\mathbf{r}}\cdot\hat{\mathbf{n}})\mathbf{I}+\hat{\mathbf{n}}\otimes\hat{\mathbf{r}}\right)-\frac{2}{r}X\left(\hat{\mathbf{r}}\otimes\hat{\mathbf{n}}-2\hat{\mathbf{r}}\otimes\hat{\mathbf{r}}\left(\hat{\mathbf{r}}\cdot\hat{\mathbf{n}}\right)\right)-\right.$$
$$\left.2\frac{dX}{dr}\hat{\mathbf{r}}\otimes\hat{\mathbf{r}}\left(\hat{\mathbf{r}}\cdot\hat{\mathbf{n}}\right)+\left(\frac{2(1-\nu)}{1-2\nu}-2\right)\left(\frac{d\Psi}{dr}-\frac{dX}{dr}-\frac{X}{r}\hat{\mathbf{r}}\otimes\hat{\mathbf{n}}\right)\right] \tag{26}$$

and r_0 is the radius of the circular domain Ω_s. Adopting the RBF interpolation scheme of Eq. 16 for displacements and considering traction vectors defined on Γ_s as independent variables interpolated with standard quadratic or linear boundary interpolation functions (Fig. 3), Eq. 24 can be written as

$$\alpha\cdot\mathbf{u}(\mathbf{y})+\int_{\Gamma_{sq}\cup L_s}\left[\mathbf{t}^*(\mathbf{y},\mathbf{x})-\mathbf{t}^c(\mathbf{y},\mathbf{x})\right]R^k(\mathbf{x})\,d\Gamma_x\cdot\mathbf{u}^k+$$
$$\int_{\Gamma_{su}}\left[\mathbf{t}^*(\mathbf{y},\mathbf{x})-\mathbf{t}^c(\mathbf{y},\mathbf{x})\right]\cdot\bar{\mathbf{u}}(\mathbf{x})\,d\Gamma_x=$$
$$\int_{\Gamma_{sq}}\left[\mathbf{u}^*(\mathbf{y},\mathbf{x})-\mathbf{u}^c(\mathbf{y},\mathbf{x})\right]\cdot\bar{\mathbf{t}}(\mathbf{x})\,d\Gamma_x+$$
$$\int_{\Gamma_{su}}\left[\mathbf{u}^*(\mathbf{y},\mathbf{x})-\mathbf{u}^c(\mathbf{y},\mathbf{x})\right]N^k(\mathbf{x})\,d\Gamma_x\cdot\mathbf{t}^k-$$
$$\rho\int_{\Omega_s}\left[\mathbf{u}^*(\mathbf{y},\mathbf{x})-\mathbf{u}^c(\mathbf{y},\mathbf{x})\right]R^k(\mathbf{x})\,d\Omega_x\cdot\ddot{\mathbf{u}}^k-$$
$$\zeta\int_{\Omega_s}\left[\mathbf{u}^*(\mathbf{y},\mathbf{x})-\mathbf{u}^c(\mathbf{y},\mathbf{x})\right]R^k(\mathbf{x})\,d\Omega_x\cdot\dot{\mathbf{u}}^k \tag{27}$$

where $\mathbf{u}^k, \mathbf{t}^k$ are the time dependent nodal displacement and traction vectors, Γ_{su}, Γ_{st} represent parts of the global boundary where displacements $\bar{\mathbf{u}}$ and tractions $\bar{\mathbf{t}}$, respectively, are prescribed, R^k stands for the RBF interpolation functions given by Eq. 16 and N^k corresponds to the standard boundary interpolation functions.

Writing Eq. 27 in the form

$$\alpha\mathbf{u}(\mathbf{y})+\tilde{\mathbf{H}}_q^k\cdot\mathbf{u}^k+\tilde{\mathbf{H}}_L^k\cdot\mathbf{u}^k+\bar{\mathbf{H}}_u=\bar{\mathbf{G}}_q+\tilde{\mathbf{G}}_u^k\cdot\mathbf{q}^k-\rho\tilde{\mathbf{V}}^k\cdot\ddot{\mathbf{u}}^k-\zeta\tilde{\mathbf{V}}^k\cdot\dot{\mathbf{u}}^k \tag{28}$$

and replacing the first and second time derivatives of displacements by the finite difference type expressions of the implicit time integration scheme of θ - Wilson [Bathe (1996)], i.e.

$$\begin{aligned}
\ddot{u}^{t+\theta\Delta t} &= \frac{6}{\theta^2\Delta t^2}\left(u^{t+\theta\Delta t}-u^t\right)-\frac{6}{\theta\Delta t}\dot{u}^t-2\ddot{u}^t \\
\dot{u}^{t+\theta\Delta t} &= \frac{3}{\theta\Delta t}\left(u^{t+\theta\Delta t}-u^t\right)-2\dot{u}^t-\frac{\theta\Delta t}{2}\ddot{u}^t
\end{aligned} \tag{29}$$

one obtains

$$\begin{aligned}
&\left[\alpha\mathbf{I}+\tilde{\mathbf{H}}_q^k+\tilde{\mathbf{H}}_L^k+\frac{1}{\theta\Delta t}\left(\frac{6\rho}{\theta\Delta t}+3\zeta\right)\tilde{\mathbf{V}}^k\right]\cdot\mathbf{u}^{k,t+\theta\Delta t}-\tilde{\mathbf{G}}_u^k\cdot\mathbf{q}^{k,t+\theta\Delta t}= \\
&-\bar{\mathbf{H}}_u^{t+\theta\Delta t}+\bar{\mathbf{G}}_q^{t+\theta\Delta t}+\rho\tilde{\mathbf{V}}^k\left[\frac{6}{\theta^2\Delta t^2}\mathbf{u}^t+\frac{6}{\theta\Delta t}\dot{\mathbf{u}}^t+2\ddot{\mathbf{u}}^t\right]+ \\
&\zeta\tilde{\mathbf{V}}^k\left[\frac{3}{\theta\Delta t}\mathbf{u}^t+2\dot{\mathbf{u}}^t+\frac{\theta\Delta t}{2}\ddot{\mathbf{u}}^t\right]
\end{aligned} \tag{30}$$

or

$$\mathbf{A}\cdot\mathbf{u}^{t+\theta\Delta t}+\mathbf{H}\cdot\mathbf{u}^{t+\theta\Delta t}-\mathbf{G}\cdot\mathbf{t}^{t+\theta\Delta t}=\mathbf{F}^{t+\theta\Delta t} \tag{31}$$

with θ being a parameter of the time stepping scheme receiving the specific value $\theta=1.4$ for stability and accuracy [Bathe (1996)]. It is apparent that Eq. 31 has the same form with the corresponding one in a typical BEM formulation where displacements and tractions are independent variables. The difference here is the local nature of Eq. 31, which leads to a banded system of algebraic equations and not to a fully populated system as in BEM. By applying Eq. 31 for all nodes, imposing the boundary conditions Eq. 20 and rearranging the system coefficients, the final algebraic system of equations is obtained

$$\tilde{\mathbf{A}}\cdot\mathbf{X}=\mathbf{b} \tag{32}$$

where the vector $\mathbf{X}$ consists of all the unknown nodal displacements and boundary tractions for the time moment $t+\theta\Delta t$. Finally, by solving the above system of equations with an LU decomposition solver, the nodal values of displacements and boundary tractions are provided. After the solution for the time moment $t+\theta\Delta t$ is obtained, the displacements, tractions, velocities and accelerations for the time moment $t+\Delta t$ are computed using the following formulas [Bathe (1996)]

$$\begin{aligned}
\ddot{u}^{t+\Delta t} &= \ddot{u}^t+\frac{1}{\theta}\left(\ddot{u}^{t+\theta\Delta t}-\ddot{u}^t\right) \\
\dot{u}^{t+\Delta t} &= \dot{u}^t+\Delta t\ddot{u}^t+\frac{\Delta t}{2\theta}\left(\ddot{u}^{t+\theta\Delta t}-\ddot{u}^t\right) \\
u^{t+\theta\Delta t} &= u^t+\Delta t\dot{u}^t+\frac{1}{2}\Delta t^2\ddot{u}^t+\frac{\Delta t^2}{6\theta}\left(\ddot{u}^{t+\theta\Delta t}-\ddot{u}^t\right)
\end{aligned} \tag{33}$$

4 Indirect FFT/ MLPG(LBIE) formulation

Consider again the linear and isotropic elastic domain of the previous section. By applying the exponential Fast Fourier Transform (FFT) to the equation of motion (Eq. 19) and the corresponding boundary conditions (Eq. 20) one obtains

$$\mu\nabla^2\mathbf{u}(\mathbf{y},\omega)+(\lambda+\mu)\nabla\nabla\cdot\mathbf{u}(\mathbf{y},\omega)+\omega(\rho\omega+j\zeta)\mathbf{u}(\mathbf{y},\omega)=\mathbf{0} \tag{34}$$

and

$$\begin{aligned}\mathbf{u}(\mathbf{y},\omega)&=\bar{\mathbf{u}}(\mathbf{y},\omega),\mathbf{y}\in\Gamma_u\\ \mathbf{t}(\mathbf{y},\omega)&=\bar{\mathbf{t}}(\mathbf{y},\omega),\mathbf{y}\in\Gamma_t\end{aligned} \tag{35}$$

where $j=(0,-1)$ is the imaginary unit and ω the frequency of the Fourier transform, which is imaginary for the reasons explained later. By considering the static fundamental solution of Eq. 34 and employing the Betti's reciprocal identity, one obtains the following LBIE for the circular domain centered at any interior or boundary point $\mathbf{y}$ (Fig. 2).

$$\begin{aligned}\alpha\mathbf{u}(\mathbf{y})+\int_{\Gamma_s\cup L_s}\mathbf{t}^*(\mathbf{y},\mathbf{x})\cdot\mathbf{u}(\mathbf{x})\,d\Gamma_x=\int_{\Gamma_s\cup L_s}\mathbf{u}^*(\mathbf{y},\mathbf{x})\cdot\mathbf{t}(\mathbf{x})\,d\Gamma_x+\\ \omega(\rho\omega+j\zeta)\int_{\Omega_s}\mathbf{u}^*(\mathbf{y},\mathbf{x})\cdot\mathbf{u}(\mathbf{x})\,d\Omega_x\end{aligned} \tag{36}$$

where $\mathbf{u}^*,\mathbf{t}^*$ represent the static fundamental solution tensors of displacements and tractions given by Eq. 22 and Eq. 23. By taking into account the companion solution Eq. 25 and Eq. 26, the LBIE Eq. 36 becomes

$$\begin{aligned}\alpha\mathbf{u}(\mathbf{y})+\int_{\Gamma_s\cup L_s}[\mathbf{t}^*(\mathbf{y},\mathbf{x})-\mathbf{t}^c(\mathbf{y},\mathbf{x})]\cdot\mathbf{u}(\mathbf{x})\,d\Gamma_x=\\ \int_{\Gamma_s}[\mathbf{u}^*(\mathbf{y},\mathbf{x})-\mathbf{u}^c(\mathbf{y},\mathbf{x})]\cdot\mathbf{t}(\mathbf{x})\,d\Gamma_x+\\ \omega(\rho\omega+j\zeta)\int_{\Omega_s}[\mathbf{u}^*(\mathbf{y},\mathbf{x})-\mathbf{u}^c(\mathbf{y},\mathbf{x})]\cdot\mathbf{u}(\mathbf{x})\,d\Omega_x\end{aligned} \tag{37}$$

By adopting the RBF interpolation scheme of Eq. 16 for displacements and considering traction vectors on Γ_s as independent variables interpolated with standard linear or quadratic boundary interpolation functions (Fig. 3), Eq. 37 obtains the

form

$$\alpha \mathbf{u}(\mathbf{y}) + \int_{\Gamma_{sq} \cup L_s} [\mathbf{t}^*(\mathbf{y},\mathbf{x}) - \mathbf{t}^c(\mathbf{y},\mathbf{x})] R^k(\mathbf{x})\, d\Gamma_x \cdot \mathbf{u}^k + \int_{\Gamma_{su}} [\mathbf{t}^*(\mathbf{y},\mathbf{x}) - \mathbf{t}^c(\mathbf{y},\mathbf{x})] \cdot \bar{\mathbf{u}}(\mathbf{x})\, d\Gamma_x = \int_{\Gamma_{sq}} [\mathbf{u}^*(\mathbf{y},\mathbf{x}) - \mathbf{u}^c(\mathbf{y},\mathbf{x})] \cdot \bar{\mathbf{t}}(\mathbf{x})\, d\Gamma_x + \int_{\Gamma_{su}} [\mathbf{u}^*(\mathbf{y},\mathbf{x}) - \mathbf{u}^c(\mathbf{y},\mathbf{x})] N^k(\mathbf{x})\, d\Gamma_x \cdot \mathbf{t}^k + \omega(\rho\omega + j\zeta) \int_{\Omega_s} [\mathbf{u}^*(\mathbf{y},\mathbf{x}) - \mathbf{u}^c(\mathbf{y},\mathbf{x})] R^k(\mathbf{x})\, d\Omega_x \cdot \mathbf{u}^k \tag{38}$$

or

$$\alpha \cdot \mathbf{u}_\omega(\mathbf{x}) + \tilde{\mathbf{H}}_q^k \cdot \mathbf{u}_\omega^k + \tilde{\mathbf{H}}_L^k \cdot \mathbf{u}_\omega^k + \bar{\mathbf{H}}_{u_\omega} = \bar{\mathbf{G}}_{q_\omega} + \tilde{\mathbf{G}}_u^k \cdot \mathbf{t}_\omega^k + \omega(\rho\omega + j\zeta)\, \tilde{\mathbf{V}}^k \cdot \mathbf{u}_\omega^k \tag{39}$$

or

$$\mathbf{K}_\omega \cdot \mathbf{u}_\omega - \mathbf{G} \cdot \mathbf{t}_\omega = \mathbf{F}_\omega \tag{40}$$

where $\mathbf{u}_\omega^k, \mathbf{t}_\omega^k$ are the harmonic nodal displacement and traction vectors.

As it was previously mentioned Eq. 40 has the same form with the system of equations in a typical frequency domain BEM formulation where displacements and tractions are independent variables. However the system of algebraic equations Eq. 32 is banded and not fully populated as in the BEM. By applying Eq. 40 for all nodes, imposing the boundary conditions Eq. 35 and rearranging the system coefficients the algebraic system of equations Eq. 32 is obtained. This system can be solved by an LU decomposition solver and the nodal values of displacements and boundary tractions are calculated for all frequencies of the FFT spectrum. Finally the time history of all fields is obtained via the inverse FFT.

It should be mentioned here that for minimizing the aliasing phenomena, the exponential window method proposed by [Kausel and Roësset (1992)] is adopted, where complex frequencies with a small imaginary part of the form $\omega_c = \omega - jc$ are used. The constant c is equal to $0.7\Delta\omega$, where $\Delta\omega$ is the frequency step. After solving numerically the problem in the frequency domain and then applying the inverse Fourier transform, the time response is rescaled with the aid of the exponential factor.

5 Numerical examples

The achieved accuracy of the MLPG(LBIE)/RBF method illustrated in the previous sections is demonstrated in the present section with the solution of three representative transient elastic problems.

5.1 Rectangle under uniform tension

The first problem concerns the uniform tension of a 2m ×4m rectangle by a step load of 1 Pa as it is depicted in Fig. 4. The considered material properties, i.e.

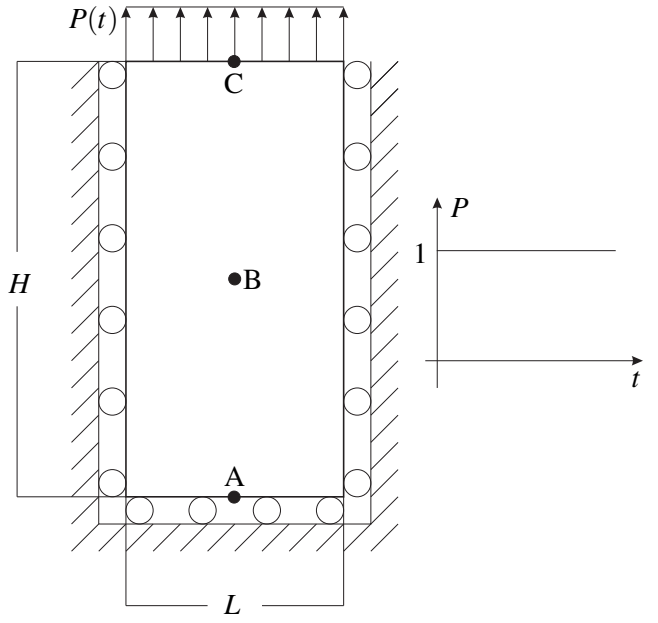

Figure 4: Rectangle under uniform step-type tension.

Young modulus, Poisson ratio, mass density and damping coefficient are E=100000 Pa, $\nu = 0.25$, $\rho = 1\text{Kg/m}^3$ and $\zeta = 0$, respectively. 2701 nodes (37×73) have been used for the solution of the problem, while the support domains have been considered to be the same for all the points and equal to 0.1333 m. In the direct time domain MLPG(LBIE)/RBF formulation the time step Δt of the θ - Wilson scheme is 0.0067 s, while in the FFT-MLPG(LBIE)/RBF formulation 128 FFT points for the time of 0.15 s have been considered. The displacement at points B and C, the traction at point A and the normal stress σ_{yy} at point B are shown in Fig. 5, Fig. 6, Fig. 7 and Fig. 8, respectively. The obtained results are compared to the analytical ones provided in the book of [Dominguez (1993)]. Observing the plots of Fig. 5-Fig. 8, one can say that the results taken by the FFT - MLPG(LBIE) formulation seem to be more accurate than these obtained by the direct time domain - MLPG(LBIE) scheme.

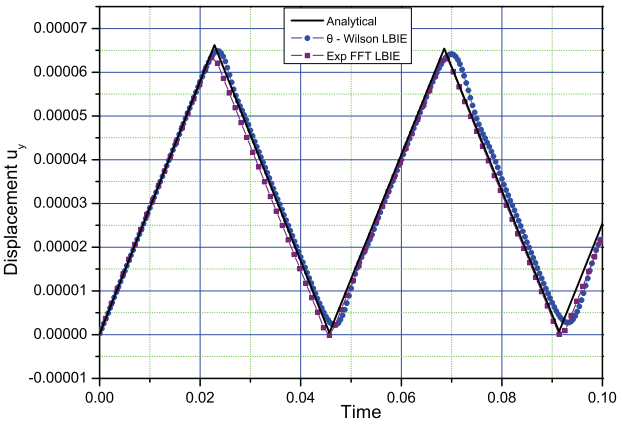

Figure 5: Time history of vertical displacement u_y, at the point C(1, 4) illustrated in Fig. 4.

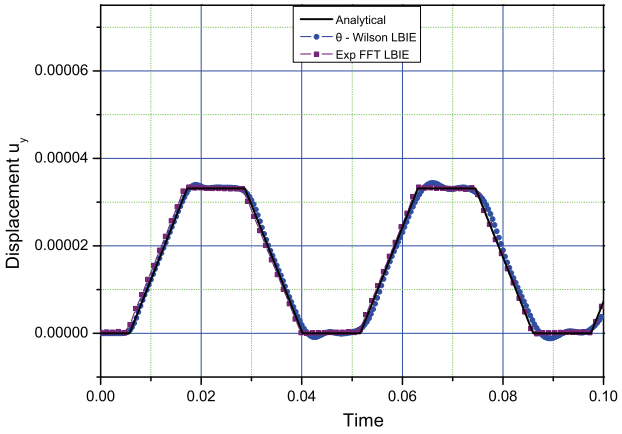

Figure 6: Time history of vertical displacement u_y, at the point B(1, 2) illustrated in Fig. 4.

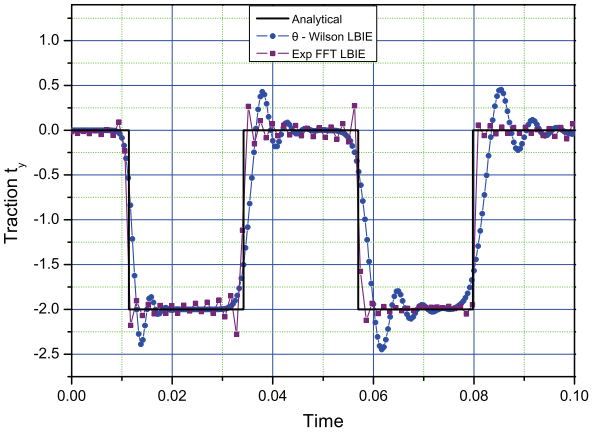

Figure 7: Time history of normal traction component t_y, at the point A(1, 0) illustrated in Fig. 4.

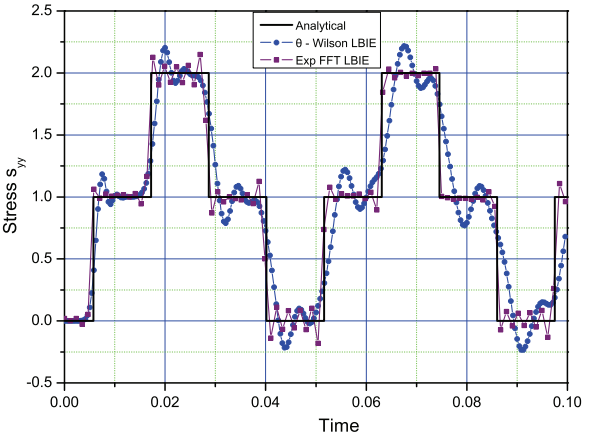

Figure 8: Time history of normal stress σ_{yy}, at the point B(1, 2) illustrated in Fig. 4.

In the sequel, the same problem with damping coefficient $\zeta = 10$ Ns/m has been solved and the time history of traction component t_y shown for $\zeta = 0$ in Fig. 7, is presented in Fig. 9. The effect of damping on the obtained results is apparent.

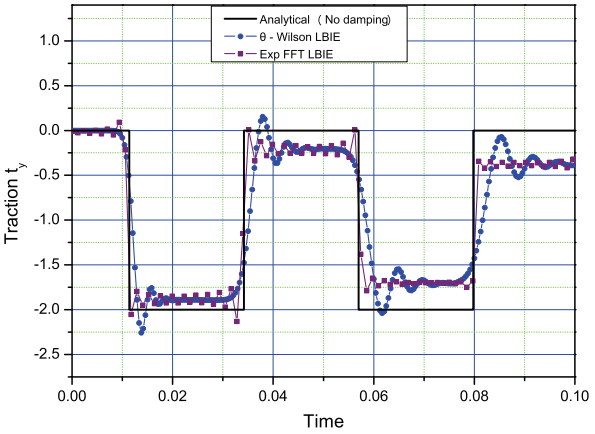

Figure 9: Time history of normal traction component t_y, at the point A(1, 0) illustrated in Fig. 4. The damping coefficient is $\zeta = 10$ Ns/m.

5.2 Hollow cylinder subjected to an internal pressure - case 1

A hollow cylinder subjected to a step load internal pressure of 1 Pa (Fig. 10 (a)) is considered. The material properties are $E = 94.6769$ Pa, $\nu = 0.2308$, $\rho = 1\text{Kg/m}^3$ and $\zeta = 0$. The inner and outer diameters of the cylinder have been taken equal to 1m and 9.4m, respectively. Due to the symmetry of the problem, only one half was modeled. The cylinder has been discretized with 4015 nodes and their arrangement is shown in Fig. 10 ($n_r = 55$, $n_\theta = 73$). The support domains are the same for the nodal points having the same radial distance from the center of the cylinder. Thus the minimum and the maximum radii of the support domains considered in the present problem are 0.304 m and 0.984 m, respectively. In the direct time domain-MLPG(LBIE) formulation the time step Δt of the θ - Wilson scheme, has been taken equal to 0.00631s, while in the FFT-MLPG(LBIE) formulation 64 FFT points for the time of 1.15s have been considered. The time histories corresponding to the radial displacement u_r, the radial stress σ_{rr} and the angular stress $\sigma_{\theta\theta}$ of the nodal point A(2.02, 0) (Fig. 10) are demonstrated in Fig. 11, Fig. 12 and Fig. 13, respectively, and compared to the analytical and numerical results provided by [Chou and Koenig (1966)] and [Carrer and Mansur (1999)]. The conclusion here is that

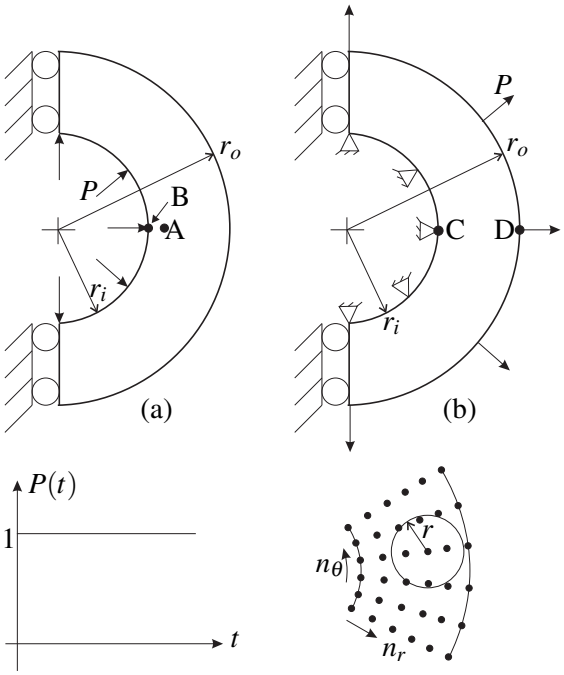

Figure 10: Hollow cylinder subjected to a stepwise internal (a) and external (b) pressure.

the agreement between numerical and analytical results is very good with the direct domain-MLPG(LBIE) results being slightly better than those obtained by the FFT-MLPG(LBIE) formulation.

5.3 Hollow cylinder subjected to an internal pressure - case 2

In the work of [Soares (2007)] the transient hollow cylinder problem of the previous section (Fig. 10 (a)) with internal pressure $p(t) = 0.22 \cdot 10^8$Pa, $r_i = 3.048$m, $r_o = 15.240$m, $E = 6.5277 \cdot 10^8$Pa, $\nu = 0.2308$, $\rho = 1804$Kg/m^3 and $\zeta = 0$ has been solved. The same problem is considered here and the internal radial displacement u_r (Fig. 10 (a), point B$(3.048, 0)$) is evaluated and compared to the one obtained by [Soares (2007)] in Fig. 14. The minimum and the maximum radii of the support domains considered in the present problem are 0.511m and 1.44m, respectively. In the direct time domain-MLPG(LBIE) formulation the time step Δt of the θ -

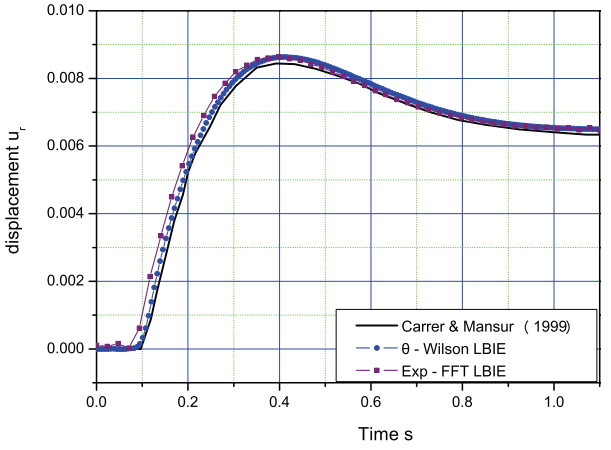

Figure 11: Time variation of radial displacement u_r, at the point A(2.02, 0) illustrated in Fig. 10 (a)

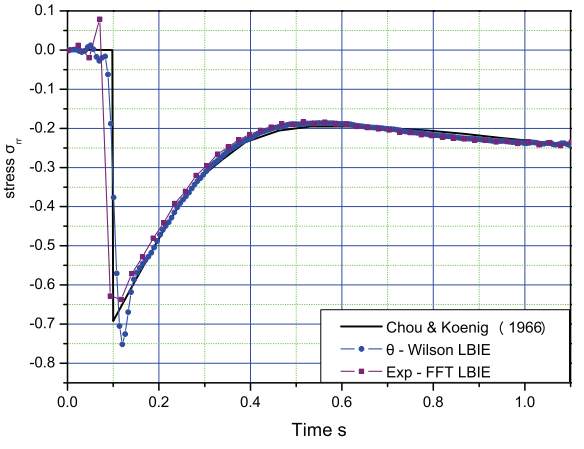

Figure 12: Time variation of radial stress σ_{rr}, at the point A(2.02, 0) illustrated in Fig. 10 (a)

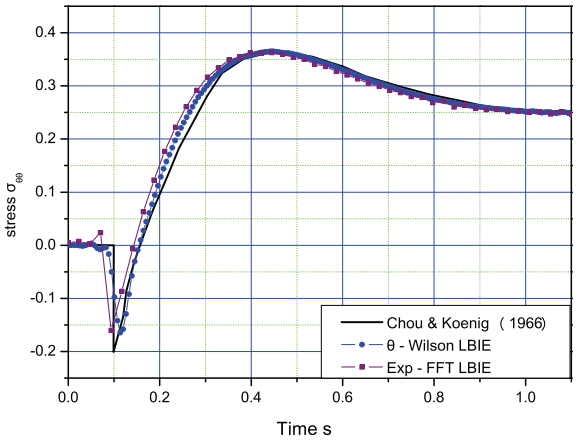

Figure 13: Time variation of angular stress $\sigma_{\theta\theta}$, at the point A(2.02, 0) illustrated in Fig. 10 (a)

Wilson scheme, is equal to 0.000459s, while in the FFT-MLPG(LBIE) formulation 256 FFT points for the time of 0.45s have been considered. 3969 total nodes are used with $n_r = 49, n_\theta = 81$ (Fig. 10).

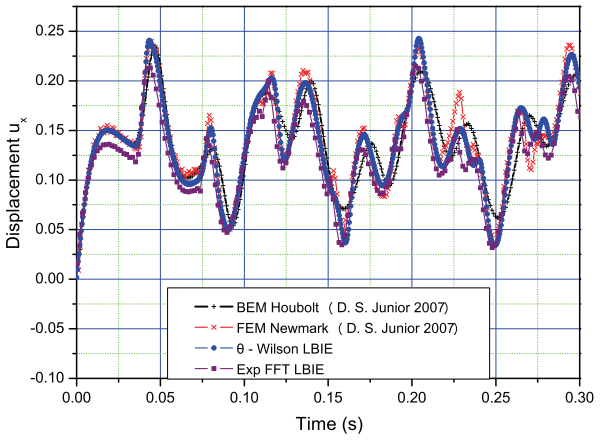

Figure 14: Time variation of inner radial displacement u_r, at the point B(3.048, 0) illustrated in Fig. 10 (a)

5.4 Hollow cylinder subjected to an external pressure

Finally, [Frangi and Novati (1999)] using a time domain BEM solved the previous transient problem considering a cylinder with very large internal and external radii subjected to an external radial tension. The interesting point of this problem is that its solution is the same with the rectangle in tension described in section 5.1. Here the problem has been solved for $p(t) = 1\text{Pa}$, $r_i = 200\text{m}$, $r_o = 204\text{m}$, $E = 100000\text{Pa}$, $\nu = 0.25$, $\rho = 1\text{Kg/m}^3$ and $\zeta = 0$. The time history of the radial traction t_r and the radial displacement u_r at the points C(200, 0) and D(204, 0) (Fig. 10 (b)), respectively, have been evaluated and compared to the analytical solution of the problem. The corresponding diagrams are shown in Fig. 15 and Fig. 16. 28519 total nodes are used with $n_r = 19, n_\theta = 1501$ (Fig. 10). The minimum and the maximum radii of the support domains are 1.0074m and 1.0254m, respectively. The time step of the θ-Wilson scheme is $\Delta t = 0.000555\text{s}$ and in the FFT-MLPG(LBIE) formulation 128 FFT points for the time of 0.15s have been considered.

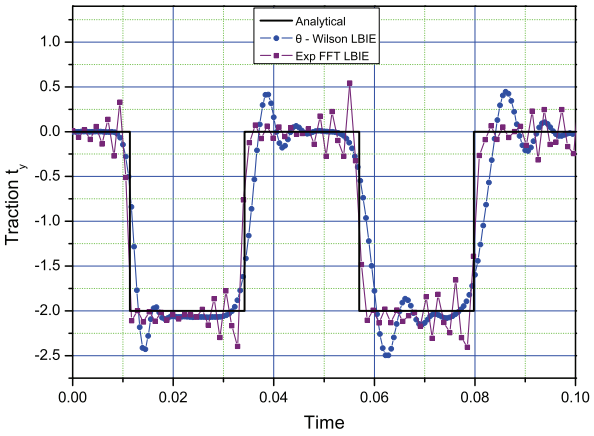

Figure 15: Time history of radial traction t_r at the point C(200, 0) illustrated in Fig. 10 (b)

6 Conclusions

A meshless local boundary integral equation (LBIE) method for solving two dimensional transient elastodynamic problems with and without damping has been proposed. For the meshless representation of displacements throughout the analyzed domain, the local Radial Basis Functions (RBF) interpolation scheme is employed. On the intersections between the local domains and the global boundary,

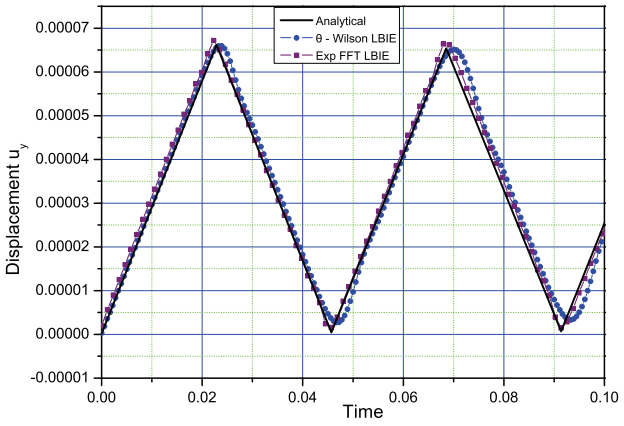

Figure 16: Time history of radial displacement u_r at the point D(204, 0) illustrated in Fig. 10 (b)

tractions are treated as independent variables via boundary interpolation functions, thus avoiding derivatives of RBF interpolation functions. The method is applied to both transient and steady-state Fourier transform domains. More precisely, the θ-Wilson finite difference scheme is exploited for the treatment of acceleration and velocity terms in the transient version of the method, while for the indirect solution of transient problems an efficient direct and inverse Fast Fourier Transform technique is employed. The achieved accuracy of the proposed methodology is assessed with the solution of three representative benchmarks. On the basis of the obtained results, the following conclusions can be drawn:

- The method works with a very good accuracy in both transient and steady-state Fourier transform elastodynamic domains.
- Comparing the results obtained in the present work with those taken by [Sellountos and Polyzos (2005b)], one can say that both techniques provide similar accuracy. However, the meshless LBIE methodology proposed in [Sellountos and Polyzos (2005b)] uses the MLS approximation scheme for the meshless representation of displacements and tractions and thus, due to the lack of delta property, it works only for uniform distribution of points.
- In the paper of [Vavourakis, Sellountos, and Polyzos (2006)], one of the conclusions was that meshless LBIE methods employing MLS approximation schemes are more accurate than those based on RBFs. This inconsistency with the present work is due to the treatment of displacements and trac-

tions on the global boundary. More precisely, in [Vavourakis, Sellountos, and Polyzos (2006)] the RBF interpolation of a boundary parameter was accomplished with the neighboring boundary points only and not with all points (boundary plus the internals) belonging to the support domain of the considered node, a fact that decreases the accuracy of RBF interpolation scheme.

Acknowledgement: This work has been supported by the Research Project PTDC/MAT/68166/2006, the Center of Mathematics and its Applications (CEMAT) through FCT's Funding Program and by the grant SFRH/BPD/27225/2006 of FCT (E.J.Sellountos).

References

Agnantiaris, J.; Polyzos, D.; Beskos, D. (1998): Three dimensional vibration analysis by the Dual Reciprocity BEM. *Computational Mechanics*, vol. 21, pp. 372–381.

Atluri, S. (2004): *The meshless method (MLPG) for domain & BIE discretizations*. Tech Science Press.

Atluri, S.; Han, Z.; Shen, S. (2003): Meshless local Petrov-Galerkin (MLPG) approaches for solving the weakly singular traction and displacement boundary integral equations. *CMES: Computer Modeling in Engineering & Sciences*, vol. 4, pp. 507–517.

Atluri, S.; Sladek, J.; Sladek, V.; Zhu, T. (2000): The local boundary integral equation (LBIE) and its meshless implementation for linear elasticity. *Computational Mechanics*, vol. 25, pp. 180–198.

Atluri, S. N.; Shen, S. (2002): The meshless local Petrov-Galerkin (MLPG) method: A simple and less-costly alternative to the finite and boundary element method. *Computer Methods in Applied Mechanics and Engineering*, vol. 3, pp. 11–51.

Atluri, S. N.; Shen, S. P. (2002): *The meshless local Petrov-Galerkin (MLPG) method*. Tech. Science Press.

Atluri, S. N.; Zhu, T. (1998): A new meshless local Petrov-Galerkin (MLPG) approach in computational mechanics. *Computational Mechanics*, vol. 22, pp. 117–127.

Bathe, K. (1996): *Finite element procedures*. Prentice Hall, New Jersey.

Beskos, D. (1987): Boundary element methods in dynamic analysis. *Applied Mechanics Reviews*, vol. 40, pp. 1–23.

Beskos, D. (1997): Boundary element methods in dynamic analysis. Part II. *Applied Mechanics Reviews*, vol. 50, pp. 149–197.

Bodin, A.; Ma, J.; Xin, X.; Krishnaswami, P. (2006): A meshless integral method based on regularized boundary integral equation. *Computer Methods in Applied Mechanics and Engineering*, vol. 195, pp. 6258–6286.

Carrer, J.; Mansur, W. (1999): Stress and velocity in 2D transient elastodynamic analysis by the boundary element method. *Engineering Analysis with Boundary Elements*, vol. 23, pp. 233–245.

Chou, P.; Koenig, H. (1966): A Unified Approach to Cylindrical and Spherical Elastic Waves by Method of Characteristics. *Journal of Applied Mechanics, TRANS. ASME*, vol. 23, pp. 159–167.

Dominguez, J. (1993): *Boundary Elements in Dynamics*. CMP, Southampton and Elsevier Applied Sience, London.

Durbin, F. (1974): Numerical inversion of Laplace transforms: an efficient improvement to Dubner and Abate's method. *Computer Journal*, vol. 17, pp. 371–376.

Emdadi, A.; Kansa, E.; Libre, N.; Rahimian, M.; Shekarchi, M. (2008): Stable PDE Solution Methods for Large Multiquadric Shape Parameters. *CMES: Computer Modeling in Engineering & Sciences*, vol. 25 (1), pp. 23–42.

Frangi, A.; Novati, G. (1999): On the numerical stability of time - domain elastodynamic analyses by BEM. *Computer Methods in Applied Mechanics and Engineering*, vol. 173, pp. 403–417.

Gosz, S.; Liu, W. (1996): Admissible approximations for essential boundary conditions in the reproducing kernel particle method. *Computational Mechanics*, vol. 19, pp. 120–135.

Han, Z.; Atluri, S. N. (2003): On simple formulations of weaklysingular traction & displacement BIE, and their solutions through Petrov Galerkin approaches. *CMES: Computer Modeling in Engineering & Sciences*, vol. 4, pp. 5–20.

Han, Z. D.; Atluri, S. N. (2007): A Systematic Approach for the Development of Weakly–Singular BIEs. *CMES: Computer Modeling in Engineering & Sciences*, vol. 21 (1), pp. 41–52.

Hardy, R. (1990): Theory and applications of the multiquadrics-biharmonic method (20 years of discovery 1968–1988). *Computers and Mathematics with Applications*, vol. 19, pp. 163–208.

Kausel, E.; Roësset, J. (1992): Frequency domain analysis of undamped systems. *Journal of Engineering Mechanics ASCE*, vol. 118, pp. 721–734.

Kosec, G.; Sarler, B. (2008): Local RBF Collocation Method for Darcy Flow. *CMES: Computer Modeling in Engineering & Sciences*, vol. 25 (3), pp. 197–208.

Le, P.; Mai-Duy, N.; Tran-Cong, T.; Baker, G. (2008): A Meshless Modeling of Dynamic Strain Localization in Quasi-Brittle Materials Using Radial Basis Function Networks. *CMES: Computer Modeling in Engineering & Sciences*, vol. 25 (1), pp. 43–68.

Libre, N.; Emdadi, A.; Kansa, E.; Rahimian, M.; Shekarchi, M. (2008): A stabilized RBF collocation scheme for Neumann type boundary value problems. *CMES: Computer Modeling in Engineering & Sciences*, vol. 24 (1), pp. 61–80.

Libre, N. A.; Emdadi, A.; Kansa, E. J.; Shekarchi, M.; Rahimian, M. (2008): A Fast Adaptive Wavelet scheme in RBF Collocation for nearly singular potential PDEs. *CMES: Computer Modeling in Engineering & Sciences*, vol. 38 (3), pp. 263–284.

Ma, Q. (2008): A New Meshless Interpolation Scheme for MLPG_R Method. *CMES: Computer Modeling in Engineering & Sciences*, vol. 23 (2), pp. 75–90.

Manolis, G.; Beskos, D. (1981): Dynamic stress concentration studies by boundary integrals and Laplace transform. *International Journal for Numerical Methods in Engineering*, vol. 17, pp. 573–599.

Manolis, G.; Beskos, D. (1988): *Boundary Element Methods in Elastodynamics*. Unwin Hyman, London.

Mohammadi, M. (2008): Stabilized Meshless Local Petrov-Galerkin (MLPG) Method for Incompressible Viscous Fluid Flows. *CMES: Computer Modeling in Engineering & Sciences*, vol. 29 (2), pp. 75–94.

Nardini, D.; Brebbia, C. (1983): Transient dynamic analysis by the boundary element method. *In: Brebbia CA, Futagami T, Tanaka M, (Eds), Boundary Elements, Springer, Berlin, Heidelberg New York*, vol. 50, pp. 719–730.

Orsini, P.; Power, H.; Morvan, H. (2008): Improving Volume Element Methods by Meshless Radial Basis Function Techniques. *CMES: Computer Modeling in Engineering & Sciences*, vol. 23 (2), pp. 187–208.

Polyzos, D.; Tsinopoulos, S.; Beskos, D. (1998): Static and dynamic boundary element analysis in incompressible linear elasticity. *European Journal of Mechanics - A/Solids*, vol. 17, pp. 515–536.

Sellountos, E.; Polyzos, D. (2005): A MLPG (LBIE) approach in combination with BEM. *Computer Methods in Applied Mechanics and Engineering*, vol. 194, pp. 859–875.

Sellountos, E.; Sequeira, A. (2008): A hybrid multi-region BEM / LBIE-RBF velocity-vorticity scheme for the two-dimensional Navier-Stokes equations. *CMES: Computer Modelling in Engineering and Sciences*, vol. 23 (2), pp. 127–148.

Sellountos, E.; Sequeira, A. (2008): An advanced meshless LBIE/RBF method for solving two dimensional incompressible fluid flows. *Computational Mechanics*, vol. 41 (5), pp. 617–631.

Sellountos, E.; Vavourakis, V.; Polyzos, D. (2005): A new Singular/Hypersingular MLPG (LBIE) method for 2D elastostatics. *CMES: Computer Modeling in Engineering & Sciences*, vol. 7 (1), pp. 35–48.

Sellountos, E. J.; Polyzos, D. (2003): A MLPG (LBIE) method for solving frequency domain elastic problems. *CMES: Computer Modelling in Engineering & Sciences*, vol. 4, pp. 619–636.

Sellountos, E. J.; Polyzos, D. (2005): A meshless local boundary integral equation method for solving transient elastodynamic problems. *Computational Mechanics*, vol. 35 (4), pp. 265–276.

Sladek, J.; Sladek, V.; Atluri, S. (2002): Application of the local boundary integral equation method to boundary value problems. *International Journal of Applied Mechanics*, vol. 38, pp. 1025–1043.

Sladek, J.; Sladek, V.; Atluri, S.; Keer, R. V. (2000): Numerical integration of singularities of local boundary integral equations. *Computational Mechanics*, vol. 25, pp. 394–403.

Sladek, J.; Sladek, V.; Keer, R. V. (2003): Meshless local boundary integral equation method for 2D elastodynamic problems. *International Journal of Numerical Methods in Engineering*, vol. 57, pp. 235–249.

Sladek, V.; Sladek, J.; Tanaka, M. (2005): Local integral equations and two meshless polynomial interpolations with application to potential problems in Non-

homogeneous Media. *CMES: Computer Modeling in Engineering & Sciences*, vol. 7 (1), pp. 69–84.

Sladek, V.; Sladek, J.; Zhang, C. (2006): Comparative study of meshless approximations in local integral equation method. *CMC: Computers, Materials & Continua*, vol. 4 (3), pp. 177–188.

Sladek, V.; Sladek, J.; Zhang, C. (2008): Computation of stresses in non-homogeneous elastic solids by local integral equation method: a comparative study. *Computational Mechanics*, vol. 41, pp. 827–845.

Soares, D. J. (2007): A time-marching scheme based on implicit Green's functions for elastodynamic analysis with the domain boundary element method. *Computational Mechanics*, vol. 40 (5), pp. 827–853.

Vavourakis, V. (2008): A Local Hypersingular Boundary Integral Equation Method Using a Triangular Background Mesh. *CMES: Computer Modeling in Engineering & Sciences*, vol. 36 (2), pp. 119–146.

Vavourakis, V.; Polyzos, D. (2007): A new MLPG(LBIE) method for solving 2D elastostatic problems. *Computers Materials and Continua*, vol. 5 (3), pp. 185–196.

Vavourakis, V.; Polyzos, D. (2008): A MLPG(LBIE) numerical method for solving 2D incompressible and nearly incompressible elastostatic problems. *Communications in Numerical Methods in Engineering*, vol. 24, pp. 281–296.

Vavourakis, V.; Sellountos, E.; Polyzos, D. (2006): A comparison study on different MLPG(LBIE) formulations. *CMES: Computer Modeling in Engineering & Sciences*, vol. 13, pp. 171–184.

Wang, J.; Liu, G. (2002): A point interpolation meshless method based on radial basis functions. *International Journal of Numerical Methods in Engineering*, vol. 54 (11), pp. 1623–1648.

Wang, J.; Liu, G. (2002): On the optimal shape parameters of radial basis functions used for 2-D meshless methods. *Computer Methods in Applied Mechanics in Engineering*, vol. 191 (23-24), pp. 2611–2630.

Wen, P.; Aliabadi, M.; Liu, Y. (2008): Meshless Method for Crack Analysis in Functionally Graded Materials with Enriched Radial Base Functions. *CMES: Computer Modeling in Engineering & Sciences*, vol. 30 (3), pp. 133–147.

Zhu, T.; Zhang, J.-D.; Atluri, S. N. (1998): A local boundary integral equation (LBIE) method in computational mechanics, and a meshless discretization approach. *Computational Mechanics*, vol. 21 (3), pp. 223–235.